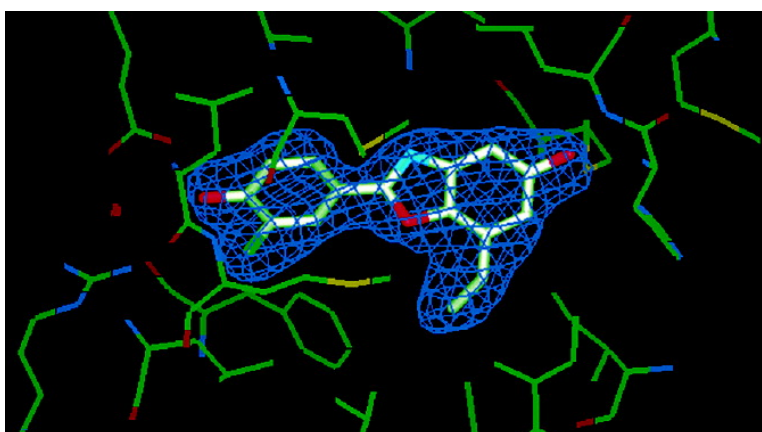Article

Structure-Based Design of Estrogen Receptor-β Selective Ligands

Eric S. Manas, Rayomand J. Unwalla, Zhang B. Xu, Michael S. Malamas, Chris P. Miller,
Heather A. Harris, Chulai Hsiao, Tatos Akopian, Wah-Tung Hum, Karl Malakian, Scott Wolfrom,
Ashok Bapat, Ramesh A. Bhat, Mark L. Stahl, William S. Somers, and Juan C. Alvarez

More About This Article

Additional resources and features associated with this article are available within the HTML version:

- Supporting Information
- Links to the 8 articles that cite this article, as of the time of this article download
- Access to high resolution figures
- Links to articles and content related to this article
- Copyright permission to reproduce figures and/or text from this article

View the Full Text HTML

Structure-Based Design of Estrogen Receptor-β Selective Ligands

Eric S. Manas,*,† Rayomand J. Unwalla,† Zhang B. Xu,‡ Michael S. Malamas,§
Chris P. Miller,⊥ Heather A. Harris,‖ Chulai Hsiao,‡ Tatos Akopian,#
Wah-Tung Hum,‡ Karl Malakian,‡ Scott Wolfrom,‡ Ashok Bapat,‖ Ramesh A. Bhat,‖
Mark L. Stahl,‡ William S. Somers,‡ and Juan C. Alvarez▽

*Contribution from the Department of Chemical and Screening Sciences, Wyeth Research,
500 Arcola Road, Collegeville, Pennsylvania 19426; Department of Chemical and Screening
Sciences, Wyeth Research, 200 Cambridge Park Drive, Cambridge, Massachusetts 02140;
Department of Chemical and Screening Sciences, Wyeth Research,
Monmouth Junction, New Jersey 08852; Women's Health Research Institute,
Wyeth Research, 500 Arcola Road, Collegeville, Pennsylvania 19426*

Received April 23, 2004; E-mail: manase@wyeth.com

Abstract: We present the structure-based optimization of a series of estrogen receptor-β (ERβ) selective ligands. X-ray cocrystal structures of these ligands complexed to both ERα and ERβ are described. We also discuss how molecular modeling was used to take advantage of subtle differences between the two binding cavities in order to optimize selectivity for ERβ over ERα. Quantum chemical calculations are utilized to gain insight into the mechanism of selectivity enhancement. Despite only two relatively conservative residue substitutions in the ligand binding pocket, the most selective compounds have greater than 100-fold selectivity for ERβ relative to ERα when measured using a competitive radioligand binding assay.

Introduction

Estrogen receptors (ERs) are ligand activated transcription factors. The primary endogenous ligand for these receptors is 17β-estradiol (E2), which is normally produced by the ovaries or through peripheral metabolism of precursor hormones (e.g., testosterone). However, ERs can also bind a diverse range of synthetic agonists and antagonists. In the past several years, it has been shown that certain compounds behave as ER agonists in some tissues and ER antagonists in others. These compounds with mixed activity are called selective estrogen receptor modulators (SERMS; for review, see ref 1). The precise reason the same compound can have cell-specific effects has not been elucidated, but differences in receptor conformation, co-regulatory proteins, and promoters have all been suggested.

A major advance toward understanding the differential effects of various estrogenic compounds came with the recent discovery of an additional form of the estrogen receptor.[2] The second isoform, called ERβ, is similar in sequence to the previously known isoform, now called ERα. Mapping the distribution of ERβ and ERα mRNA in normal and neoplastic tissues has provided an intriguing picture of differential expression patterns in different tissue types.[3−6] The existence of clear-cut differences in receptor expression suggests that tissues could be differentially targeted with receptor selective ligands. In particular, the fact that ERβ is widely expressed but not the dominant estrogen receptor in uterus or breast tissues has made it a very attractive drug target. However, until very recently,[7] any specific therapeutic utility of an ERβ selective ligand has been unclear. As described in ref 7, availability of highly selective ligands has enabled us to probe the physiological function of ERβ. For example, the ERβ selective agonist ERB-041 was used to demonstrate that this receptor may be a useful target for certain inflammatory diseases,[7] while similar studies utilizing the ERα selective agonist propylpyrazole triol (PPT) showed that many classical estrogenic effects are mediated by ERα.[8] In the current

† Department of Chemical and Screening Sciences, Wyeth Research, Pennsylvania.

‡ Department of Chemical and Screening Sciences, Wyeth Research, Massachusetts.

§ Department of Chemical and Screening Sciences, Wyeth Research, New Jersey.

‖ Women's Health Research Institute, Wyeth Research, Pennsylvania.

⊥ Present address: GlaxoSmithKline, Corporate Intellectual Property, King of Prussia, PA 19406.

Present address: Department of Biochemistry, AstraZeneca Research and Development, 35 Gatehouse Drive, Waltham, MA 02451.

▽ Present address: Transform Pharmaceuticals, 29 Hartwell Avenue, Lexington, MA 02421.

(1) McDonnell, D. P. *Journal of the Society for Gynecologic Investigation* **2000**, *7*, S10−S15.

(2) Kuiper, G.; Enmark, E.; Pelto Huikko, M.; Nilsson, S.; Gustafsson, J. A. *Proceedings of the National Academy of Sciences of the United States of America* **1996**, *93*, 5925−5930.

(3) Couse, J. F.; Lindzey, J.; Grandien, K.; Gustafsson, J. A.; Korach, K. S. *Endocrinology* **1997**, *138*, 4613−4621.

(4) Shughrue, P. J.; Komm. B.; Merchenthaler. I. *Steroids* **1996**, *61*, 678−681.

(5) Lau, K. M.; Leav, I.; Ho, S. M. *Endocrinology* **1998**, *139*, 424−427.

(6) Enmark, E.; Peltohuikko, M.; Grandien, K.; Lagercrantz, S.; Lagercrantz, J.; Fried, G.; Nordenskjold, M.; Gustafsson, J. A. *Journal of Clinical Endocrinology and Metabolism* **1997**, *82*, 4258−4265.

(7) Harris, H. A.; Albert, L. M.; Leathurby, Y.; Malamas, M. S.; Mewshaw, R. E.; Miller, C. P.; Kharode, Y. P.; Marzolf, J.; Komm, B. S.; Winneker, R. C.; Frail, D. E.; Henderson, R. A.; Zhu, Y.; James C.; Keith, J. *Endocrinology* **2003**, *144*, 4241−4249.

(8) Harris, H. A.; Katzenellenbogen, J. A.; Katzenellenbogen, B. S. *Endocrinology* **2002**, *143*, 4172−4177.

paper we discuss our structure-based design approach to the design of highly ERβ selective agonists, which, along with traditional medicinal chemistry studies, has helped provide us with valuable tools such as ERB-041 to help elucidate the physiological role of ERβ.

Like other nuclear receptors, estrogen receptors have a modular structure consisting of six discrete domains designated A−F. These domains mediate binding to DNA, ligands, and other proteins (e.g., coactivators).[9,10] The E domain (ligand binding domain or "LBD") of ER binds ligands such as E2 and the phytoestrogen, genistein (GEN). Whereas E2 binds to both ERα and ERβ with similar affinity, phytoestrogens such as GEN have modest selectivity for the β-subtype, having 10−40-fold greater affinity for ERβ than for ERα.[2,11−13] Although the existence of naturally occurring ERβ selective ligands is both fortuitous and encouraging, the modest selectivity seen for phytoestrogens is not sufficient to validate ERβ as a target.

Another major advance, which has paved the way for structure-based design of ERβ selective ligands, was the X-ray structure determination of the ERβ LBD complexed with GEN.[14] This structure clearly showed that, although ERα and ERβ are 58% identical in sequence, in actuality there are only two residue substitutions in close proximity to bound agonists: ERα Leu$_{384}$ is replaced by ERβ Met$_{336}$, and ERα Met$_{421}$ is replaced by ERβ Ile$_{373}$. Given the conservative nature of these substitutions, it is not surprising that compounds such as E2 are nonselective, while the phytoestrogens achieve only modest selectivity. In fact, although it was suggested that the ERα Met$_{421}$→ ERβ Ile$_{373}$ substitution may allow ERβ to accommodate more polar substituents,[14] so far there has been no clear explanation for the observed selectivity of phytoestrogens such as GEN.

The design of highly ERβ selective ligands has thus far proved to be quite challenging. Recently, several groups, including our own, have reported attempts to design ERβ selective ligands utilizing various scaffolds (e.g., biphenyls,[15] tetrahydrochrysenes (THC),[16−18] diarylpropionitriles (DPN),[19,20] arylbenzothiophenes,[21] isoxazoles,[22,23] benzothiazoles/benzoxazoles,[24,25] benzimidazoles,[26] triazines,[27] isoquinolines/isoindolines,[28] steroidal[29] and phytoestrogen analogues[30−32]). While some of these efforts have been successful at enhancing ERβ selectivity beyond 50-fold, many of the resulting compounds

have been on the order of 10−30-fold selective based on receptor binding. Several arguments of how compounds achieve selectivity have been presented, mostly based on docking calculations and mutation studies. However, to our knowledge, there have been no arguments presented supported by multiple X-ray structures within a congeneric series of ligands or by X-ray structures of the same molecule cocrystallized with both human ERβ and ERα.

In this paper we describe X-ray crystallographic studies and structure-based optimization of a series of ERβ selective ligands. Using ab initio quantum mechanics, we demonstrate that certain functional groups incorporated during lead optimization are able to experience a differential interaction with ERα Met$_{421}$ relative to ERβ Ile$_{373}$ on the basis of both electrostatic and dispersive effects. Furthermore, we show that taking advantage of this residue substitution affords compounds with >100-fold ERβ binding selectivity relative to ERα.
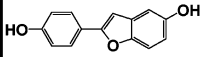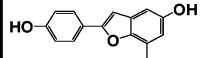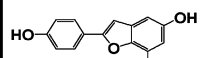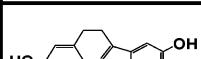
Materials and Methods
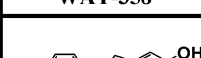
Materials. Coactivator peptide fragments, Biotin-SGSHKLVQLLTTT-COOH and Biotin-SGHKILHRLLQEG-COOH were obtained from the Wyeth DNA and peptide synthesis lab. The two peptides used in this study were derived from the steroid receptor coactivator 1 and 3 (SRC-1 and SRC-3) NR box domains. SRC-1 and SRC-3 are both known to enhance ligand-dependent transcriptional activation of the estrogen receptor and have been shown to be specifically recruited by agonist-bound ERβ and ERα, respectively.[33,34]

All ligands studied in this paper were obtained from the Wyeth compound library. Preparation of ERB-041 and related benzoxazole/benzofuran compounds are described elsewhere.[35−37] Binding affinities (as measured by IC$_{50}$ in a solid-phase competitive radioligand binding assay using ER LBD and [^{3}H]-17β-E2)[11] for all compounds are provided in Table 1.

(9) Tsai, M. J.; O'Malley, B. W. *Annual Review of Biochemistry* **1994**, *63*, 451−486.
(10) Evans, R. M. *Science.* **1988**, *240*, 889−895.
(11) Harris, H. A.; Bapat, A. R.; Gonder, D. S.; Frail, D. E. *Steroids* **2002**, *67*, 379−384.
(12) Kuiper, G.; Lemmen, J. G.; Carlsson, B.; Corton, J. C.; Safe, S. H.; Vandersaag, P. T.; Vanderburg, P.; Gustafsson, J. A. *Endocrinology* **1998**, *139*, 4252−4263.
(13) Kuiper, G.; Carlsson, B.; Grandian, K.; Enmark, E.; Haggblad, J.; Nilsson, S.; Gustafsson, J. A. *Endocrinology* **1997**, *138*, 863−870.
(14) Pike, A. C. W.; Brzozowski, A. M.; Hubbard, R. E.; Bonn, T.; Thorsell, A. G.; Engstrom, O.; Ljunggren, J.; Gustafsson, J. K.; Carlquist, M. *EMBO Journal* **1999**, *18*, 4608−4618.
(15) Edsall, R. J.; Harris, H. A.; Manas, E. S.; Mewshaw, R. E. *Bioorganic and Medicinal Chemistry* **2003**, *11*, 3457−3474.
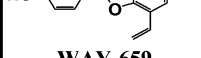(16) Meyers, M. J.; Sun, J.; Carlson, K. E.; Katzenellenbogen, B. S.; Katzenellenbogen, J. A. *Journal of Medicinal Chemistry* **1999**, *42*, 2456−2468.
(17) Sun, J.; Meyers, M. J.; Fink, B. E.; Rajendran, R.; Katzenellenbogen, J. A.; Katzenellenbogen, B. S. *Endocrinology* **1999**, *140*, 800−804.
(18) Shiau, A. K.; Barstad, D.; Radek, J. T.; Meyers, M. J.; Nettles, K. W.; Katzenellenbogen, B. S.; Katzenellenbogen, J. A.; Agard, D. A.; Greene, G. L. *Nature Structural Biology* **2002**, *9*, 359−364.
(19) Meyers, M. J.; Sun, J.; Carlson, K. E.; Marriner, G. A.; Katzenellenbogen, B. S.; Katzenellenbogen, J. A. *Journal of Medicinal Chemistry* **2001**, *44*, 4230−4251.
(20) Sun, J.; Baudry, J.; Katzenellenbogen, J. A.; Katzenellenbogen, B. S. *Molecular Endocrinology* **2003**, *17*, 247−258.
(21) Schopfer, U.; Schoeffter, P.; Bischoff, S. F.; Nozulak, J.; Feuerbach, D.; Floersheim, P. *Journal of Medicinal Chemistry* **2002**, *45*, 1399−1401.

(22) Katzenellenbogen, J. A.; Katzenellenbogen, B. S.; Fink, B. E.; Stauffer, S. R.; Mortensen, D. S.; Sattigeri, V. J.; Huang, Y. In *PCT Int. Appl.*; (Board of Trustees of the University of Illinois, USA). WO 2000019994, 2000, p 134 pp.
(23) Huebner, V. D.; Lin, X.; James, I.; Chen, L.; Desai, M.; Moore, J. C.; Krywult, B.; Navaratnam, T.; Singh, R.; Trainor, R.; Wang, L. In *PCT Int. Appl.*; (Chiron Corporation, USA). WO 2000008001, 2000, p 115 pp.
(24) Barlaam, B.; Bernstein, P.; Dantzman, C.; Warwick, P. In *PCT Int. Appl.*; (Astrazeneca AB, Swed.). WO 2002051821, 2002, p 71 pp.
(25) Bernstein, P. In *PCT Int. Appl.*; (Astrazeneca A. B., Swed.). WO 2003045930, 2003, p 30 pp.
(26) Barlaam, B.; Dock, S.; Folmer, J. In *PCT Int. Appl.*; (Astrazeneca AB, Swed.). WO 2002046168, 2002, p 46 pp.
(27) Henke, B. R.; Consler, T. G.; Go, N.; Hale, R. L.; Hohman, D. R.; Jones, S. A.; Lu, A. T.; Moore, L. B.; Moore, J. T.; Orband-Miller, L. A.; Robinett, R. G.; Shearin, J.; Spearing, P. K.; Stewart, E. L.; Turnbull, P. S.; Weaver, S. L.; Williams, S. P.; Wisely, G. B.; Lambert, M. H. *Journal of Medicinal Chemistry* **2002**, *45*, 5492−5505.
(28) Barlaam, B.; Dantzman, C. In *PCT Int. Appl.*; (Astrazeneca AB, Swed.). WO 2002046164, 2002, p 44 pp.
(29) Hegele-Hartung, C.; Siebel, P.; Peters, O.; Kosemund, D.; G, M. A. l.; Hillisch, A.; Walter, A.; Kraetzschmar, J.; Fritzemeier, K. H. *Proceedings of the National Academy of Sciences of the United States of America* **2004**, *101*, 5129−5134.
(30) Barlaam, B. C.; Piser, T. M. In *PCT Int. Appl.*; (Astrazeneca AB, Swed.). WO 2000062765, 2000, p 23 pp.
(31) Barlaam, B.; Folmer, J. J.; Piser, T. M. In *PCT Int. Appl.*; (Astrazeneca AB, Swed.). WO 2002030407, 2002, p 36 pp.
(32) Miller, C. P.; Collini, M. D.; Harris, H. A. *Bioorganic and Medicinal Chemistry Letters* **2003**, *13*, 2399−2403.
(33) Wong, C. W.; Komm, B.; Cheskis, B. J. *Biochemistry* **2001**, *40*, 6756−6765.
(34) Heery, D. M.; Hoare, S.; Hussain, S.; Parker, M. G.; Sheppard, H. *Journal of Biological Chemistry* **2001**, *276*, 6695−6702.
(35) Malamas, M. S.; Manas, E. S.; McDevitt, R. E.; Gunawan, I.; Xu, Z. B.; Collini, M. D.; Miller, C. P.; Dinh, T.; Henderson, R. A.; Keith, J. C., Jr.; Harris, H. A. *J. Med. Chem.* **2004**, *47*, 5021−5040.
(36) Miller, C. P.; Collini, M. D.; Kaufman, D. H.; Morris, R. L.; Singhaus, R. R., Jr.; Ullrich, J. W.; Harris, H. A.; Keith, J. C., Jr.; Albert, L. M.; Unwalla, R. J. In *PCT Int. Appl.*; (Wyeth, John, and Brother Ltd., USA). WO 2003051860, 2003, p 103 pp.
(37) Collini, M. D.; Kaufman, D. H.; Manas, E. S.; Harris, H. A.; Henderson, R. A.; Xu, Z. B.; Unwalla, R. J.; Miller, C. P. *Bioorg. Med. Chem. Lett.* **2004**, *14*, 4925−4929.

Table 1. Binding Affinity (As Measured by IC$_{50}$) of Compounds Studied in This Paper[a]

Ligand	ERβ IC$_{50}$ (nM)	(LCL, UCL)	N	ERα IC$_{50}$ (nM)	(LCL, UCL)	N	Selectivity	(LCL, UCL)
WAY-397	5.7	(5.0, 6.4)	32	161.9	(138.4, 189.2)	31	28.6	(23.5, 34.9)
WAY-697	1.9	(1.2, 2.9)	9	65.3	(36.3, 117.6)	9	34.6	(17.7, 67.8)
WAY-244	14.0	(11.3, 17.4)	8	1062.5	(754.3, 1496.6)	8	75.8	(52.5, 109.6)
WAY-358	1.1	(0.8, 1.5)	6	176.8	(97.8, 319.7)	7	157.0	(83.7, 294.7)
WAY-354	3.9	(2.9, 5.2)	10	79.8	(58.8, 108.2)	10	20.5	(16.1, 26.2)
WAY-818	46.7	(37.5, 58.2)	10	1129.9	(835.6, 1527.7)	10	24.2	(17.1, 34.2)
WAY-292	5.5	(4.4, 7.0)	7	391.1	(283.8, 538.9)	7	70.9	(49.8, 101.0)
WAY-659	3.0	(1.9, 4.7)	9	385.6	(239.9, 619.6)	9	127.3	(70.0, 231.5)
ERB-041	4.1	(2.8, 5.9)	21	1048.8	(808.3, 1361.0)	20	255.5	(191.9, 340.1)

[a] Lower and upper 95% confidence limits (LCL, UCL) are reported for the geometric mean of N IC$_{50}$ determinations and were calculated using statistical methods described in the text.

Cloning, Expression, and Purification of Human ERβ LBD. Human ERβ cDNA was generated from human testis RNA by RT-PCR and cloned into mammalian expression vector pcDNA3. Amino acids 261−500 were amplified from the cloned cDNA by PCR with the forward primer 5′-GAACCATGGACGACGCCCTGAGCCCCGAG-CAGCTAGTG-3′ and the reverse primer 5′-GGACTCGAGTTAGTCGT-CAAGCACGTGGGCATTCAGCATCTC-3′. The PCR fragment was inserted into *E. coli* expression vector pET16b (Novagen) between the NcoI and XhoI restriction sites. The primers used encode three extra asp codons, one before the codon for D$_{261}$ and two after L$_{500}$. The expressed LBD thus has the following sequence: MD[D261-L500]-DD. ERβ LBD was overexpressed from a high-density culture of *E. coli* BL21DE3 host cells (Stratagene).

The ERβ LBD was purified as follows. Harvested cells were lysed by two cycles of French press (SLM Instrument) at 20 000 psi in a buffer of 20 mM Tris-Cl pH 7.5, 0.5 M NaCl, 5 mM DTT, and 1 mM EDTA (10 mL/g of cells). Clarified lysate was flowed through a Q Sepharose (Pharmacia) column and then applied to a 5 mL estradiol-Sepharose fast flow column (PTI Research, Inc) and washed with 300 mL of 10 mM Tris-HCL, pH 7.5 containing 0.5 M NaCl and 1 mM EDTA (buffer A). The column was then re-equilibrated with 50 mL of 10 mM Tris-HCl, pH 7.5, 0.2 M NaCl, and 1 mM EDTA (buffer B),

and then the protein was carboxymethylated using 50 mL of buffer B containing 5 mM iodoacetic acid. Then the column was washed by 500 mL of buffer A, followed by elution in buffer A containing 50–200 μM ligand. The final step was size exclusion chromatography (Sephadex 200, Pharmacia) using the elution buffer containing 5 μM ligand. Excess ligand was finally removed by passing the solution through a G-25 column (Pharmacia).

Cloning, Expression, and Purification of Human ERα LBD. Amino acids 301–554 were amplified from human ovaries total RNA by RT-PCR using a forward primer of 5′-GAATTCTCATGAGTAA-GAAGAACAGCCTGGCCTT-3′ and a reverse primer of 5′-AGTTG-GATCCTCGAGTCAGCTAGTGGGCGCATGTAGGCG-3′. The amplification product was gel purified and digested with Rca I and Xho I for the purpose of cloning into pET16b. This fragment was introduced into pET16b that had been digested with NcoI and XhoI. Transformants containing the correct plasmid sequence were used for ERα LBD expression. The expressed ERα LBD has the following sequence: $M[S_{301}-S_{554}]$. The ERα LBD was overexpressed from a high-density culture of *E. coli* BL21DE3-RP host cells (Stratagene).

The ERα LBD was purified by resuspending the cell pellet in a buffer of 100 mM Tris-HCl pH 8.5, 100 mM KCl, 1 mM EDTA, and 4 mM DTT (10 mL/g of cells). The cell suspension was disrupted by passing through a microfluidizer 5 times (model 110Y, Microfluidics Corp). After centrifugation (13 000 × *g* 30 min, 4 °C), the pellet was extracted with 4 M urea in the same buffer. The urea extract was applied to a 5 mL estradiol-Sepharose fast flow column (PTI Research, Inc). The column was first washed with 1 M urea in the above buffer and then sequentially washed with the following: (1) 50 mM Tris-HCl pH 8.5, 700 mM KCl, 1 mM EDTA, and 1 mM DTT; (2) 50 mM Tris-HCl pH 8.5, 250 mM NaSCN, 1 mM EDTA, and 1 mM DTT in 10% dimethylformamide; (3) 10 mM Tris-HCl pH 8.0. While the ERα LBD was bound to the estradiol-affinity column, carboxymethylation was performed by equilibrating the column with 5 mM iodoacetic acid in 10 mM Tris-HCl pH 8.0 overnight at 4 °C. Protein was eluted with 100 μM ligand and desalted with a BioRad disposable desalting column equilibrated with 50 mM ammonium bicarbonate pH 7.5.

Crystallography. The ERβ/WAY-397 complex was concentrated to 12.5 mg/mL in a buffer containing 0.2 M NaCl, 1mM EDTA, 5mM DTT, and 10mM Tris-HCl at pH 7.5 and then mixed with the SRC-1 peptide at a molar ratio of 1.5:1 peptide to protein–ligand complex. Screening of crystallization conditions was performed at 18 °C using the hanging drop vapor diffusion method.[38] Crystals were grown from a drop containing a mixture of protein/ligand–peptide solution and reservoir solution of 25% PEG2000 (v/v), 0.15 M MgCl, 20 mM hexaminecobalt trichloride, and 0.1 M MES, pH 6.0.

The ERβ/WAY-244 complex was concentrated to 10.0 mg/mL in the same buffer as the ERβ/WAY-397 complex and then mixed with the SRC-1 peptide at a molar ratio of 5:1 peptide to protein–ligand complex. Crystals were grown using the same technique as those above and appeared over wells containing 15% PEG3350 (v/v) and 0.15 M magnesium formate. The crystallization conditions for ERβ/WAY-697 and ERβ/ERB-041 were similar to those for ERβ/WAY-244, except that the molar ratio of peptide to protein–ligand complex was 1.5:1.

The ERα/WAY-244 complex was concentrated to 11.0 mg/mL in a buffer containing 50 mM ammonium bicarbonate at pH 7.5 and then mixed with the SRC-3 peptide at a molar ratio of 1.5:1.0 peptide to protein–ligand complex. Crystals were grown using the same technique as that above and appeared over wells containing 15% PEG3350 (v/v), 0.2 M NaI, and 0.1 M HEPES at pH 7.4. Prior to data collection all crystals were briefly soaked in a solution containing mother liquor and 15–20% glycerol (v/v).

X-ray data were collected at 100 K using a Quantum-4 CCD area detector at the Advanced Light Source (ALS, Berkeley, CA) and processed using DENZO and Scalepack.[39] Crystal structures were solved

by molecular replacement using the program AMORE.[40] All ERβ complex structures were solved using ERβ complexed with GEN as a search model. This ERβ/GEN structure was in turn solved in-house by molecular replacement, using ERα complexed with E2 as a model[41] (pdb code: 1A52) and was later found to be in good agreement with the published structure[14] (pdb code: 1QKM). The ERα/WAY-244 complex structure was solved using ERα complexed with DES[42] (pdb code: 3ERD) as the search model. To avoid model bias, the ligand, the loop connecting H8–H9, the C and N terminal helices, and the coactivator peptide were omitted from the search models. For the ERα/WAY-244 structure, Met_{421} was also omitted from the search model. Structures were refined using the program CNS.[43] The resulting difference electron density maps show clear electron density for the compounds, residues within the binding site, helix 12, and the coactivator peptide. The final models of the ERα and ERβ complex crystal structures contain a dimer, with a ligand and coactivator peptide bound to each monomer, and a variable number of water molecules. Cysteine modifications and some flexible loop residues were not included in the models due to poor electron density. Table 2 gives the data collection and refinement details for all of the complexes studied. Atomic coordinates have been deposited in the Protein Data Bank, with accession codes 1U9E (ERβ/WAY-397), 1X76 (ERβ/WAY-697), 1X7B (ERβ/ERB-041), 1X78 (ERβ/WAY-244), and 1X7E (ERα/WAY-244).

Molecular Modeling. The docking methodology used here has been described in detail elsewhere.[15] Briefly, docking calculations were performed using the QXP software package.[44] After minimization of the X-ray ligand in the active site, constrained simulated annealing dynamics calculations were performed to relieve any artifacts of the X-ray refinement perceived as unfavorable interactions or strain by the QXP force field. Once the binding site model was generated, docking of analogues was performed using the QXP Monte Carlo docking algorithm mcdock. In general, 1000 Monte Carlo steps were sufficient for the poses and their energy scores to converge. Visualization of X-ray structures and docking results was performed using the InsightII software package (Accelrys, Inc., San Diego, CA).

All quantum chemical calculations were performed using the Jaguar software package (Jaguar 5.5; Schrodinger, LLC, Portland, OR). Intermolecular potential energy curves were calculated by constructing a z-matrix for both molecules and then varying the intermolecular distance while holding the relative orientation of the two molecules fixed. Molecular geometries were optimized at the LMP2 level of theory using the 6-311G**++ basis set.[45–48] Potential energies were then calculated for the optimized structures using the augmented correlation-consistent polarized valence triple-ζ (aug-cc-pVTZ) basis set,[49–52] also at the LMP2 level of theory. The LMP2 (local Møller–Plesset second-order perturbation theory) method was designed to incorporate the

(38) McPherson, A., Jr. *Methods of Biochemical Analysis* **1976**, *23*, 249–345.

(39) Otwinowski, Z.; Minor, W. *Methods in Enzymology* **1994**, *276*, 307–326.
(40) Bailey, S. *Acta Crystallographica, Section D: Biological Crystallography* **1994**, *50*, 760–763.
(41) Tanenbaum, D. M.; Wang, Y.; Williams, S. P.; Sigler, P. B. *Proceedings of the National Academy of Sciences of the United States of America* **1998**, *95*, 5998–6003.
(42) Shiau, A., K.; Barstad, D.; Loria Paula, M.; Cheng, L.; Kushner Peter, J.; Agard David, A.; Greene Geoffrey, L. *Cell* **1998**, *95*, 927–937.
(43) Brunger, A. *Acta Crystallographica, Section D: Biological Crystallography* **1998**, *55*, 941–944.
(44) McMartin, C.; Bohacek, R. S. *Journal of Computer-Aided Molecular Design* **1997**, *11*, 333–344.
(45) Clark, T.; Chandrasekhar, J.; Spitznagel, G. W.; Schleyer, P. v. R. *Journal of Computational Chemistry* **1983**, *4*, 294–301.
(46) Frisch, M. J.; Pople, J. A.; Binkley, J. S. *Journal of Chemical Physics* **1984**, *80*, 3265–3269.
(47) Krishnan, R.; Binkley, J. S.; Seeger, R.; Pople, J. A. *Journal of Chemical Physics* **1980**, *72*, 650–654.
(48) McLean, A. D.; Chandler, G. S. *Journal of Chemical Physics* **1980**, *72*, 5639–5648.
(49) Woon, D. E.; Dunning, T. H., Jr. *Journal of Chemical Physics* **1994**, *100*, 2975–2988.
(50) Woon, D. E.; Dunning, T. H., Jr. *Journal of Chemical Physics* **1993**, *98*, 1358–1371.
(51) Kendall, R. A.; Dunning, T. H., Jr.; Harrison, R. J. *Journal of Chemical Physics* **1992**, *96*, 6796–6806.
(52) Dunning, T. H., Jr. *Journal of Chemical Physics* **1989**, *90*, 1007–1023.

Table 2. X-ray Data Collection and Refinement Statistics for Structures Studied in This Paper

			Data Collection		
PBD ID code	1U9E	1X76	1X78	1X7B	1X7E
protein	ERβ	ERβ	ERβ	ERβ	ERα
ligand	WAY-397	WAY-697	WAY-244	ERB-041	WAY-244
space group	$P2_12_12_1$	$P2_12_12_1$	$P2_12_12_1$	$P2_12_12_1$	$P2_1$
wavelength (Å)	1.10	1.10	1.10	1.10	1.10
unit cell dimensions					
a (Å)	52.113	52.231	51.891	52.181	58.136
b (Å)	87.935	87.951	87.507	87.981	79.895
c (Å)	99.524	99.794	99.493	99.918	59.830
cell angles (°)	$\alpha = \beta = \gamma = 90$	$\alpha = \beta = \gamma = 90$	$\alpha = \beta = \gamma = 90$	$\alpha = \beta = \gamma = 90$	$\alpha = \gamma = 90, \beta = 116.19$
maximal resolution (Å)	2.4	2.2	2.3	2.3	2.8
observations	18744	23879	20125	19756	11682
completeness (%)	99.5	99.6	96.8	94.1	96.3
R_{merge} (%)[a]	7.9	5.8	6.1	6.5	12.6
mean $I/\sigma(I)$	22.3	21.8	18.8	20.1	7.36
reflections used	17999	23399	19663	19285	9623
reflections in working set	17129	22260	18696	18350	9107
reflections in test set	870	1139	967	935	516
highest resolution bin (Å)	2.44−2.40	2.24−2.20	2.34−2.30	2.38−2.30	2.90−2.80
completeness (%)	99.8	97.8%	92.9	94.2	90.7
R_{merge} (%)[a]	37.4	24.3	31.4	33.5	34.6
mean $I/\sigma(I)$	6.1	5.9	4.9	4.0	2.1
mosaicity (°)	1.086	0.618	0.821	0.907	0.500
			Refinement		
number of molecules per asymmetric unit	2	2	2	2	2
protein atoms[b]	1761/1805	1772/1772	1798/1798	1798/1773	1907/1907
other atoms					
ligand[b]	17/17	19/19	20/20	20/20	20/20
coactivator peptide[b]	71/71	71/71	71/71	81/81	96/96
water	107	112	128	140	72
resolution range (Å)	15−2.4	15−2.2	15−2.3	15−2.3	15−2.7
R_{work}[c]	0.231	0.224	0.219	0.218	0.216
R_{free}[c]	0.279	0.265	0.270	0.266	0.283
RMS bond length (Å)[d]	0.005	0.006	0.007	0.007	0.009
RMS bond angles (°)[d]	1.000	1.100	1.200	1.300	1.400
mean B-factor (Å^2)					
complex	29.5	30.4	33.6	34.1	18.4
main-chain atoms	29.2	29.9	33.3	33.4	18.3
side-chain atoms	30.0	31.0	34.2	35.4	19.4
ligand	20.9	26.2	27.8	24.6	6.0
water	29.4	32.4	35.7	34.6	9.5
RMS backbone ΔB (Å^2)[e]	0.661	0.742	0.671	1.026	1.108
%A,B,L (a,b,l,p)[f]	99.8	99.8	99.5	99.8	98.6

[a] $R_{merge} = \sum_n\sum_{hkl}|I_{hkl}{}^n - \langle I_{hkl}{}^n\rangle|/\sum_n\langle I_{hkl}{}^n\rangle$, where $I_{hkl}{}^n$ is the nth observation of reflection hkl, and $\langle I_{hkl}{}^n\rangle$ denotes an average of reflection hkl over n observations. [b] Per monomer unit. [c] Crystallographic R-factors were computed using $R_{work} = \sum_{hkl}|F_{hkl}{}^{obsd} - F_{hkl}{}^{calcd}|/\sum_{hkl}F_{hkl}{}^{obsd}$. R_{free} values were calculated in the same manner as R_{work}, except over approximately 4% of the data excluded from the refinement. [d] Root-mean-square deviation in bond length and bond angle distances from Engh and Huber ideal values. [e] Root-mean-square deviation between B-factors for bonded main chain atoms [f] Percentage of residues located in most favored (additional) regions of the Ramachandran plot as determined by PROCHECK.[81]

effects of electron correlation while minimizing basis set superposition error (BSSE), which can lead to a dimer energy that is artificially lower than the sum of two monomer energies.[53−57] Therefore, the method is ideally suited to calculate intermolecular interaction energies, without having to apply a counterpoise (CP) correction to the LMP2 term of the molecular energy. However, CP calculations are still necessary to obtain reliable energies for the Hartree−Fock (HF) term.[58,59] This was done at every intermolecular distance by calculating each fragment's HF single-point energy using the basis functions of the dimer at that intermolecular distance.

As a practical note, we do find that the 6-311G**++ basis set yields qualitatively similar results compared to aug-cc-pVTZ. However,

interaction energies tend to be lower with aug-cc-pVTZ, typically on the order of 0.5 kcal/mol lower when two molecules are in van der Waals contact. This is to be expected, since the aug-cc-pVTZ basis set is likely to do a better job saturating the dispersive component of the interaction, due to the addition of higher angular momentum polarization functions. We also point out that, in studies of the HF dimer,[60] individual components of the interaction energy tended to differ a considerable amount from the basis set limit for the commonly used basis sets such as 6-311G**. In particular, the electrostatic component at the correlated level tended to have a significant amount of error, although this was mitigated to some extent when diffuse functions (+) were added. Since we were concerned about interpreting results based on a "fortuitous cancellation of errors," we decided to report energies calculated using the aug-cc-pVTZ basis set.

Coordinates for the X-ray crystal structures of ERα complexed with E2 and DES, as well as for ERβ complexed with GEN, were taken from the Protein Databank[61] entries, 1ERE,[62] 1GWR,[63] 3ERD,[42] and 1QKM.[14] Protein overlays were performed using the homology module

(53) Pulay, P.; Saeboe, S. *Theoretica Chimica Acta* **1986**, *69*, 357−368.
(54) Saebo, S.; Pulay, P. *Journal of Chemical Physics* **2001**, *115*, 3975−3983.
(55) Saebo, S.; Pulay, P. *Annual Review of Physical Chemistry* **1993**, *44*, 213−236.
(56) Saebo, S.; Tong, W.; Pulay, P. *Journal of Chemical Physics* **1993**, *98*, 2170−2175.
(57) Saebo, S.; Pulay, P. *Journal of Chemical Physics* **1988**, *88*, 1884−1890.
(58) Boys, S. F.; Bernardi, F. *Molecular Physics* **1970**, *19*, 553−566.
(59) Gutowski, M.; Van Duijneveldt, F. B.; Chalasinski, G.; Piela, L. *Molecular Physics* **1987**, *61*, 233−247.

(60) Chalasinski, G.; Szczesniak, M. M. *Chemical Reviews* **1994**, *94*, 1723−1765.

of the InsightII software package (Insight 2000; Accelrys, Inc, San Diego, CA). After performing a preliminary structural alignment based on all alpha-carbons, we used the superimpose_aln command to generate matches based on fitting only alpha-carbons closer than 2.00 Å. This ensured that conformational changes in highly flexible regions such as loops did not exert an undesired influence on the overlays. Small molecule overlays were performed using the program Maestro (Maestro 6.0 Schrodinger, LLC, Portland, OR). Electron density maps were displayed using the Quanta software package (Quanta 2000; Accelrys, Inc, San Diego, CA).

Statistical Significance of Selectivity Differences. Ultimately, we would like to know when two selectivities are different to a certain level of confidence. This is of the utmost importance when trying to understand whether a certain interaction observed in a crystal structure is truly modulating the selectivity. To determine whether two selectivities are indeed "different", we must first understand how the ERα and ERβ potency measurements are distributed. In general, we find that the IC_{50} measurements most closely follow a log-normal distribution. Therefore, the small-sample confidence interval for n IC_{50} determinations can be determined on a logarithmic scale using the Student t-distribution:

$$\langle \ln(IC_{50}) \rangle \pm t_{\alpha/2}\left(\frac{\sigma}{\sqrt{n}}\right) \qquad (1)$$

where $\langle\ \rangle$ denotes an arithmetic mean of n measurements, σ is the standard deviation of $\ln(IC_{50})$, and $t_{\alpha/2}$ is the t value with an area of $\alpha/2$ (under the t sampling distribution) to its right, based on $n - 1$ degrees of freedom. The level of confidence is given by $100 - \alpha$. Exponentiation of the arithmetic mean of $\ln(IC_{50})$ then yields the geometric mean IC_{50}, and adding or subtracting the confidence interval before exponentiation yields the upper and lower confidence limits for the mean.

If we denote the selectivity s as a ratio of two geometric mean values $\bar{a}$ and $\bar{b}$, the selectivity on a logarithmic scale can then be written as a difference between two arithmetic means:

$$\ln(s) = \langle\ln(a)\rangle - \langle\ln(b)\rangle \qquad (2)$$

To determine a confidence interval for the selectivity, it is important to correctly propagate the degrees of freedom originating from individual potency measurements. To this end, we chose to utilize a pooled sample variance[64] to calculate the error in $\ln(s)$. The pooled sample variance σ_s^2 for $\ln(s)$ is given by

$$\sigma_s^2 = \frac{(n_a - 1)\sigma_a^2 + (n_b - 1)\sigma_b^2}{n_a + n_b - 2} \qquad (3)$$

where σ_a^2 and σ_b^2 are the sample variances of $\langle\ln(a)\rangle$ and $\langle\ln(b)\rangle$, respectively. The values n_a and n_b are the respective number of IC_{50} determinations for a and b. Equation 3 is clearly an average variance weighted by the number of degrees of freedom for each set of measurements, relative to the total number of degrees of freedom, $n_a + n_b - 2$. The confidence interval for the selectivity on a logarithmic scale is then given by

$$\left[\langle\ln(a)\rangle - \langle\ln(b)\rangle\right] \pm t_{\alpha/2}\sigma_s\sqrt{\left(\frac{1}{n_a} + \frac{1}{n_b}\right)} \qquad (4)$$

The upper and lower confidence limits for the ratio $s = \bar{a}/\bar{b}$ are then given by exponentiation of eq 4. Now that we have the variance σ_s^2 and degrees of freedom $df = n_a + n_b - 2$ for $\ln(s)$, we can compare the selectivities of two compounds, $\ln(s_1)$ and $\ln(s_2)$, and calculate the variance of the difference:

$$\sigma_{\text{diff}}^2 = \frac{df_1\sigma_{s1}^2 + df_2\sigma_{s2}^2}{df_1 + df_2} \qquad (5)$$

The confidence interval for the difference between the two selectivities on a logarithmic scale is then given by

$$\left[\ln(s_1) - \ln(s_2)\right] \pm t_{\alpha/2}\sigma_{\text{diff}}\sqrt{\left(\frac{1}{n_1} + \frac{1}{n_2}\right)} \qquad (6)$$

where n_1 and n_2 are the total number of IC_{50} determinations involved in calculating s_1 and s_2, respectively. The upper and lower confidence limits for the ratio s_1/s_2 are then calculated by exponentiation of eq 6.

Results

General Observations. The overall ERβ and ERα LBD structures are similar to those previously reported,[14,42,62,63] and thus they will not be described in detail here. We do want to comment that in all cases the helix-12 conformation corresponds to that observed for other bound agonists,[42,62,63,65] consistent with our goal of designing an ERβ selective *agonist*. Briefly, the ligand is completely excluded from the solvent by the position of helix H12, which "closes" over the binding pocket and projects the hydrophobic side chains of ERβ residues Leu491 and Leu495 (Leu539 and Leu543 in ERα) toward the bound ligand. The closing of H12 over the ligand binding pocket also forms a cavity on the surface of the LBD, formed by helices H3, H4, H5, and H12 and the turn between H3 and H4. The coactivator fragment binds to this cavity in an α-helical conformation, in a manner similar to what has been previously described for other ERα LBD complexes (see Figure 1).[42,63,65]

Unbiased electron density difference maps unambiguously define the ligand binding mode for all complexes studied, as shown in Figure 2. For all of the ligands, the phenol mimics the E2 "A-ring." In particular, the phenolic hydroxyl (4′-OH) is involved in a hydrogen bonding network between ERβ residues Glu305 and Arg346 (ERα residues Glu353 and Arg394) and a highly ordered water molecule. Another hydrogen bond is formed between the benzofuran/benzoxazole hydroxyl (5-OH) and $N_{\delta 1}$ of ERβ His475 (ERα His524). The core scaffold, consisting of the A-ring phenyl, and the benzofuran/benzoxazole B and C rings, fills the remainder of the primarily hydrophobic pocket. For WAY-397 and WAY-244, the A and B rings are approximately coplanar, while, for WAY-697 and ERB-041, the A−B ring dihedral angles differ significantly from zero (32° and 23°, respectively). Quantum mechanical evaluation of the energy with respect to the A−B ring dihedral[66] shows that the energetic profiles are similar for the 2-phenyl benzofuran and 2-phenyl benzoxazole. The minimum is near 0 °, and the energy rises somewhat slowly as the dihedral angle increases. Given the "flatness" of the potential energy curve, significantly

(61) Berman, H. M.; Westbrook, J.; Feng, Z.; Gilliland, G.; Bhat, T. N.; Weissig, H.; Shindyalov, I. N.; Bourne, P. E. *Nucleic Acids Research* **2000**, *28*, 235−242.
(62) Brzozowski, A. M.; Pike, A. C. W.; Dauter, Z.; Hubbard, R. E.; Bonn, T.; Engstrom, O.; Ohman, L.; Greene, G. L.; Gustafsson, J.-A.; Carlquist, M. *Nature* **1997**, *389*, 753−758.
(63) Warnmark, A.; Treuter, E.; Gustafsson, J. A.; Hubbard, R. E.; Brzozowski, A. M.; Pike, A. C. W. *Journal of Biological Chemistry* **2002**, *277*, 21862−21868.
(64) McClave, J. T., II; F. H. D. *Statistics*, 5th ed.; Macmillan Publishing Company: New York, 1991.
(65) Pike, A. C. W.; Brzozowski, A. M.; Hubbard, R. E. *Journal of Steroid Biochemistry and Molecular Biology* **2000**, *74*, 261−268.
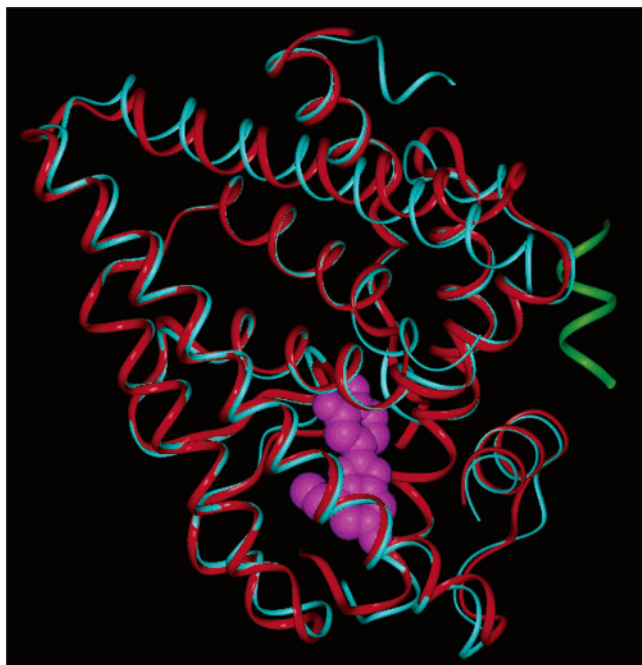(66) b3lyp/6-31G(d,p) relaxed potential energy scan.

Figure 1. Ribbon representation of ERβ (red) complexed with ERB-041 (purple) and a coactivator peptide fragment (green), overlaid with ERα (blue) complexed with 17-β estradiol (ligand not shown).

noncoplanar geometries ($\sim$20° for 2-phenyl benzoxazole, 30° for 2-phenyl benzofuran) are readily induced ($\lesssim$0.6 kcal/mol penalty) by steric interactions between the substituent at the benzofuran/benzoxazole 7-position and nearby pocket residues.

Opportunities To Improve Selectivity. Examination of the ERβ complex with WAY-397, a 29-fold ERβ selective compound, revealed a clear opportunity to improve selectivity by targeting the ERα Met$_{421}$ → ERβ Ile$_{373}$ residue substitution (see Figure 3a). As shown in Figure 3b, the 7-position of the benzofuran ring was found to overlay well with the GEN 5-OH group, which we felt might experience electrostatic repulsion with the ERα Met$_{421}$ side chain based on docking calculations and overlays with ERα/E2 or ERα/DES, thus contributing to the modest ERβ selectivity of GEN. Therefore, we felt that this would be the best position to explore with functional groups. Docking the corresponding benzoxazole WAY-818 (see Table 1) revealed a nearly perfect overlay with WAY-397, which suggested a means to access the same pocket from the analogous benzoxazole 7-position, but with significant differences in synthetic accessibility.[35]

The proximity between the GEN 5-OH group and ERα Met$_{421}$ S$_\delta$ atom alluded to above suggested to us that electronegative and chemically hard (i.e., nonpolarizable) groups would be more likely to experience a repulsive interaction with the ERα Met$_{421}$ side chain. In contrast, docking of the ERα selective ligand 16α-iodo-E2 places an iodine atom in close proximity to ERα Met$_{421}$,[67] leading us to hypothesize that aliphatic and chemically soft (i.e., polarizable) groups would be more likely to have an attractive interaction involving the S$_\delta$ atom of ERα Met$_{421}$. These both seemed like reasonable expectations due to the partial negative charge and polarizability of the methionine S$_\delta$ atom.

(67) Bhat, R. A.; Stauffer, B.; Unwalla, R. J.; Xu, Z.; Harris, H. A.; Komm, B. S. *Journal of Steroid Biochemistry and Molecular Biology* **2004**, *88*, 17–26.

For example, when a chemically hard functional group directs one or more electronegative atoms toward the S$_\delta$ atom, electrostatic repulsion is unlikely to be offset by dispersive or inductive interactions, because it would be more difficult to further induce polarization in the chemically hard group. In contrast, aliphatic and chemically soft groups (e.g., the iodine of 16α-iodo-E2) will have significant dispersive and inductive interactions with S$_\delta$, which have the potential to offset any electrostatic repulsion. These effects would not be expected with the purely hydrophobic side chain of ERβ Ile$_{373}$, making a chemically hard functional group containing electronegative atoms a more attractive synthetic target than others with regard to improving ERβ selectivity.

Quantum Chemical Calculations. Unfortunately, the balance between dispersive, inductive, and electrostatic interactions for a given functional group interacting with a residue side chain is difficult to estimate without performing ab initio quantum chemical calculations. Such calculations were quite valuable in that they allowed us to evaluate the likelihood of functional groups to have a differential interaction with ERα Met$_{421}$ versus ERβ Ile$_{373}$. For the scaffolds discussed here, we found that only groups capable of having such a differential interaction were successful at enhancing ERβ selectivity beyond 100-fold, although we point out that this differential interaction does not necessarily guarantee that the ligand will be more selective, nor is it an absolute prerequisite for a >100-fold selective ligand. For example, depending on how the functional group is presented to the pocket, it may experience unfavorable interactions with both ERα Met$_{421}$ and ERβ Ile$_{373}$. Or, if the functional group and/or ERα Met$_{421}$ can readjust in response to an unfavorable interaction without paying any significant penalty (e.g., entropic or internal strain), then it may lead to improved affinity for both isoforms. Alternatively, functional groups that do not exhibit a differential electronic interaction with ERα Met$_{421}$ relative to ERβ Ile$_{373}$ over a significant region of space could still conceivably lead to improved selectivity by virtue of differential steric repulsion or differences in contact distance (e.g., if somehow optimal contact was made with ERβ Ile$_{373}$ but not with ERα Met$_{421}$). However, we feel that there are fewer opportunities for selectivity improvement via this mechanism, given the flexibility of the methionine side chain.

Herein, we will focus on the results of quantum chemical calculations for two functional groups, nitrile and vinyl, which have been successful at enhancing ERβ selectivity beyond 100-fold when incorporated at the 7-position of the benzofuran/benzoxazole scaffold. A full SAR discussion for these scaffolds is presented elsewhere.[35,37] Figure 4a shows a schematic representation of how the functional groups and their interaction with the residue side chains were modeled. Figure 4b shows how the potential energy of CH$_3$CN varies as a function of distance from dimethyl sulfide (a model for the methionine side chain). Also shown is the potential energy curve for the same group interacting with a propyl group. Since the two curves differ only in the substitution of methylene for sulfur, this sort of analysis can help us understand which groups are most likely to experience repulsive interactions with S$_\delta$ of ERα Met$_{421}$ relative to the C$_{\gamma 1}$ of ERβ Ile$_{373}$, thus enabling the group to differentiate between the two side chains without having to take advantage of differences in size or shape. Of course, in reality
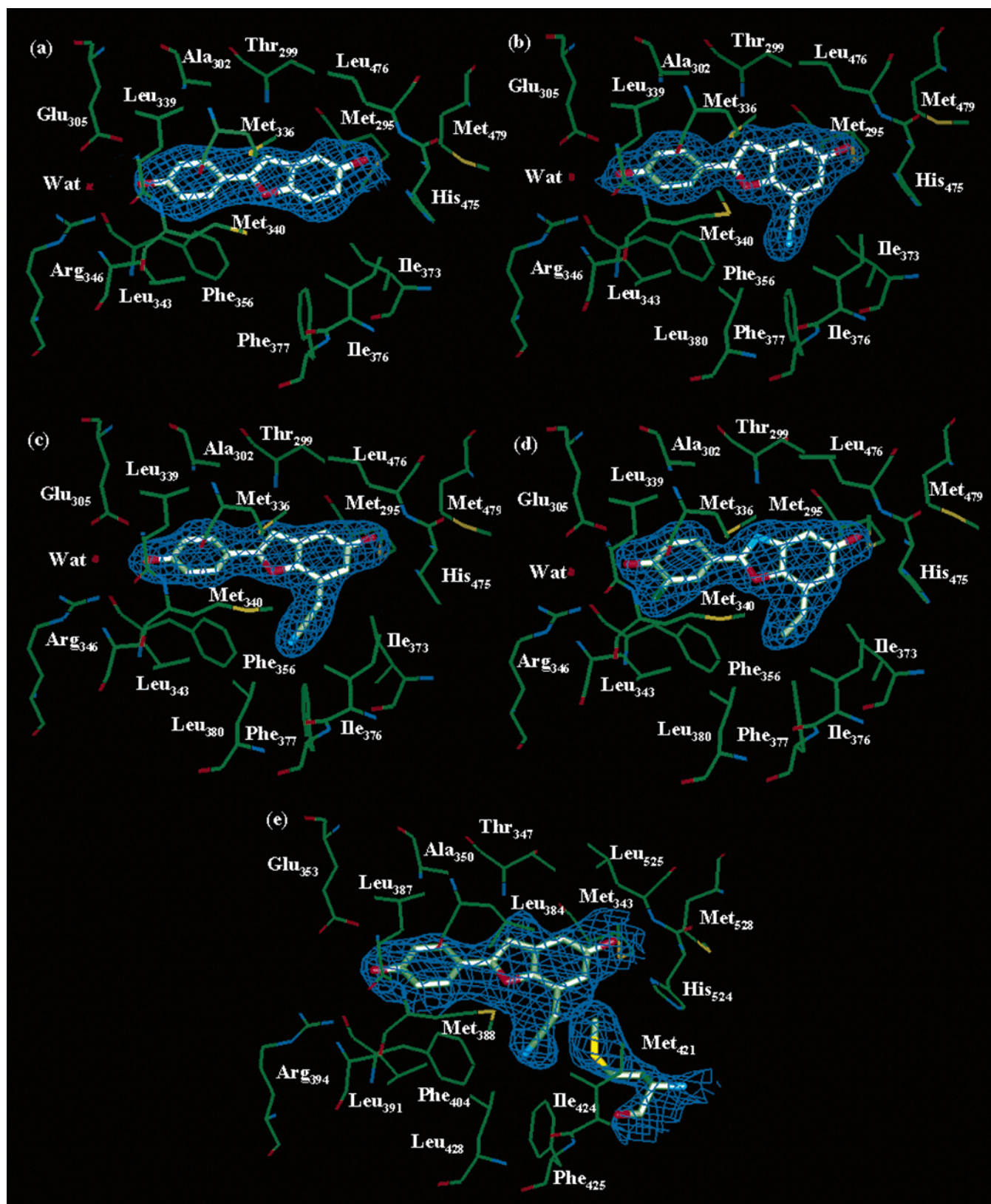
Figure 2. Unbiased $3f_o - 2f_c$ maps contoured at σ, showing the electron density for the following ligands complexed with ERβ: (a) WAY-397, (b) WAY-697, (c) WAY-244, and (d) ERB-041, as well as for (e) WAY-244 complexed with ERα. Although the crystallographic data for the ERα complex is of generally lower quality than that of the ERβ complexes, map e indicates that the binding mode of WAY-244 and the contact between the acetonitrile and Met$_{421}$ are reasonably determined by the placement of these atoms within the unbiased density.

the respective atoms of ERα Met$_{421}$ and ERβ Ile$_{373}$ also explore different regions of space; i.e., the relevant intermolecular

distances explored by the functional groups in Figure 4 might be different for ERα than for ERβ. However, since methionine
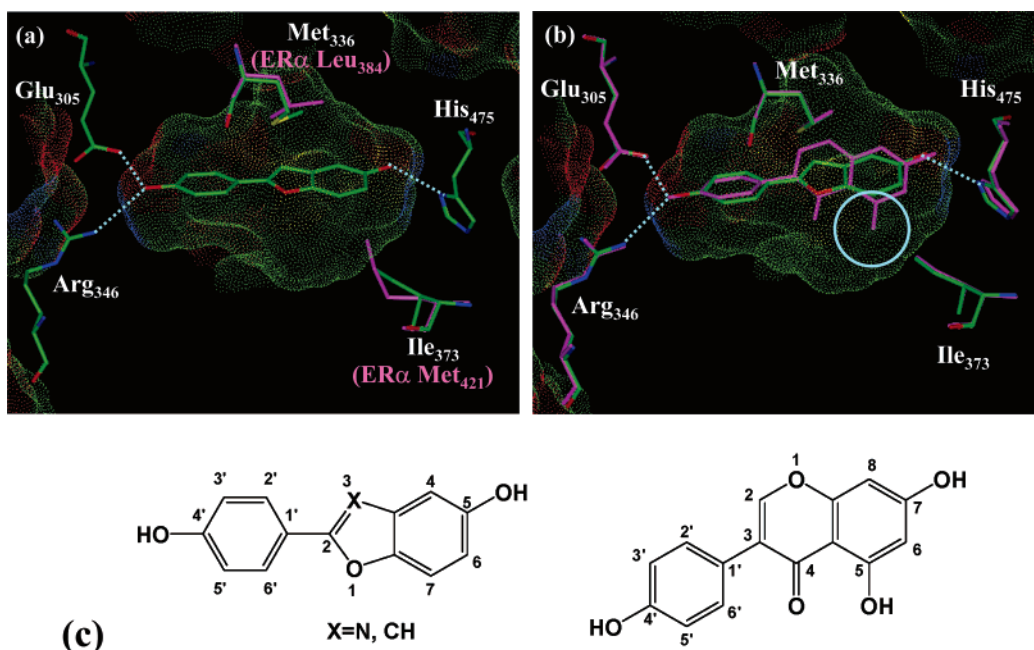
Figure 3. ERβ complexed with WAY-397 (colored by atom type), (a) overlaid with ERα/E2 (magenta, ligand not shown) and (b) overlaid with ERβ complexed with genistein (magenta). Only key residues, including a Connolly surface of the ERβ/WAY-397 binding site, are shown for simplicity. Hydrogen bonds to key residues are shown as turquoise dotted lines. The circle in part b draws attention to the correspondence between the benzofuran 7-position and the 5-OH group of genistein. (c) Numbering scheme for the benzofuran/benzoxazole scaffold and genistein. R represents the functional groups that are likely to have the greatest access to the ERα Met$_{421}$ → ERβ Ile$_{373}$ residue substitution.
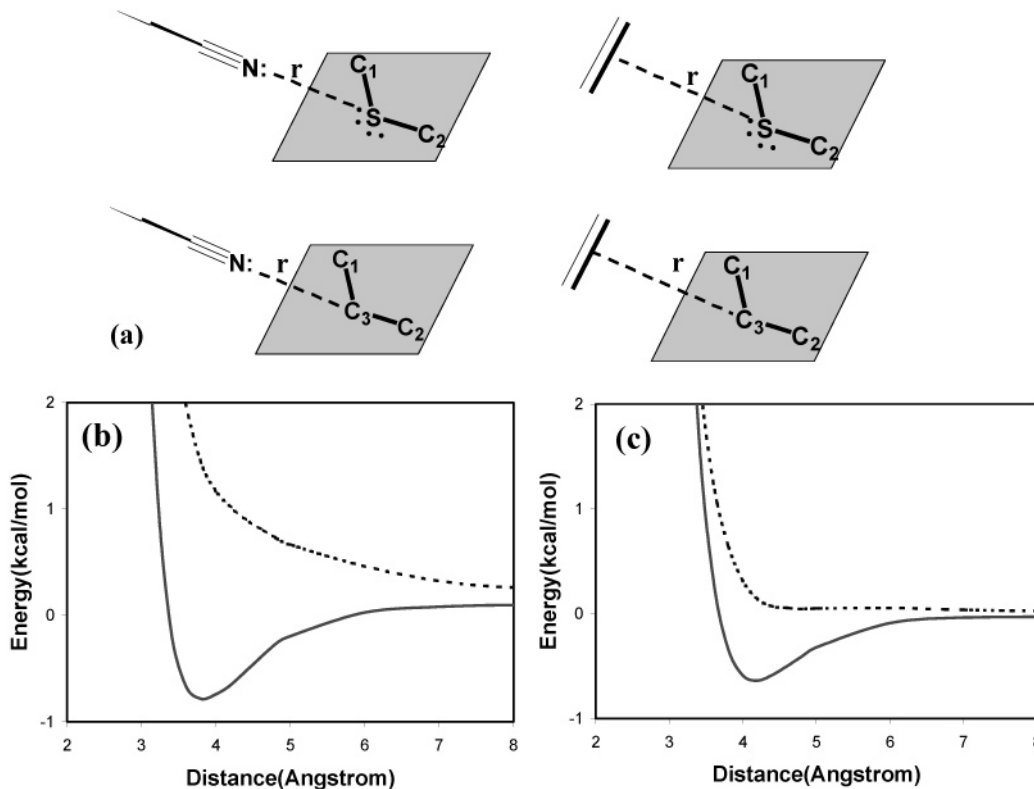
Figure 4. (a) Schematic representation of the quantum chemical calculations described in the text. Acetonitrile was oriented parallel to the line connecting the nitrogen to the sulfur/methylene carbon atom. This line was determined by constraining the N−S/C$_3$−C$_1$−C$_2$ improper dihedral to 120° and the N−S/C$_3$−C$_1$ angle to approximately 109.5°. The plane of ethylene was oriented perpendicular to the line connecting the ethylene centroid (X) and S/C$_3$, with the C−X−S/C$_3$−C$_1$ dihedral angle constrained to approximately 120°. The connecting line was determined by constraining the X−S/C$_3$−C$_1$−C$_2$ improper dihedral to 120° and the X−S/C$_3$−C$_1$ angle to approximately 109.5°. Counterpoise corrected LMP2/aug-cc-pVTZ potential energy curves are shown for (b) acetonitrile interacting with dimethyl sulfide (- - -) and propane (—) and (c) ethylene interacting with dimethyl sulfide (- - -) and propane (—).

is considered bulkier than isoleucine, this is only likely to enhance the ability of a group that already favors isoleucine over methionine to further differentiate between the two residues. Figure 4c shows similar potential energy curves for interaction with ethylene, which is used as a model for the vinyl group.

When nitrile approaches the sulfur atom end-on with the nitrogen closest to the sulfur atom, the dipole moments have a "tail-to-tail" relative orientation, which represents a purely repulsive interaction. In this case, dispersive and inductive effects are clearly not strong enough to offset the electrostatic repulsion (dipole−dipole as well as higher order), since the interaction of nitrile with dimethyl sulfide in Figure 4b is purely repulsive. Similarly, for the case of ethylene approaching the sulfur atom on its side, dispersive and inductive effects are insufficient to offset the weak electrostatic repulsion (in this case dominated by the dipole−quadrupole interaction) between the two moieties, leading to the repulsive potential energy curve shown in Figure 4c. For both ethylene and nitrile, the interaction with a propyl group is likely to be dominated by dispersive and inductive interactions and is therefore attractive in both cases.

Clearly, these results are expected to be dependent on the relative orientation of the interacting partners. For instance, nitrile can alternatively have a weakly attractive interaction with dimethyl sulfide if it approaches the sulfur atom on its side, with the C≡N: carbon and nitrogen equidistant to the sulfur atom (curve not shown). This is expected because, for a perfect "T-like" relative orientation of the nitrile and dimethyl sulfide dipoles, the dipole−dipole interaction is identically zero. Since the leading term in the electrostatic interaction is diminished, dispersion and induction can become the dominant interactions, leading to a net attraction.[68] This is consistent with the proposed mechanism of ERβ selectivity for DPN, where nitrile is believed to enhance selectivity by interacting favorably with ERβ Met$_{336}$.[19,20] The dependence of such interactions on relative orientation highlights the fact that care must be taken when designing ligands to ensure that functional groups are directed into the pocket at the appropriate angles.

7-Substituted Benzofuran and Benzoxazole Analogues. Initial attempts to enhance ERβ selectivity resulted in WAY-697, which exhibited little improvement relative to WAY-397 (see Table 1). Cocrystallization studies verified that the nitrile group of this compound extends into the small pocket formed by residues Met$_{340}$, Phe$_{356}$, Ile$_{373}$, Ile$_{376}$, Phe$_{377}$, and Leu$_{380}$, placing it in close proximity to the ERα Met$_{421}$ → ERβ Ile$_{373}$ residue substitution, as shown in Figure 2b. However, we felt that the group might not be directed into the pocket deeply enough or at the appropriate angle to lead to a significantly different interaction with ERα Met$_{421}$ relative to ERβ Ile$_{373}$. A modest enhancement in ERβ selectivity was obtained for the 7-carbonitrile benzoxazole, WAY-292 (geometric mean = 71-fold). Differences in selectivity for 7-substituted benzofuran compounds and the corresponding 7-substituted benzoxazoles can be attributed to subtle differences in scaffold geometry. This will be discussed in greater detail below.

Two strategies were utilized to direct functional groups at the benzofuran/benzoxazole 7-position more deeply into the ERα Met$_{421}$/ERβ Ile$_{373}$ pocket: (1) constraining the bond and dihedral angles that determine the relative orientation of the A and B rings and (2) inserting an sp^2 or sp^3 hybridized linker between the functional group and the benzofuran/benzoxazole ring system. Analogues utilizing both of these strategies were
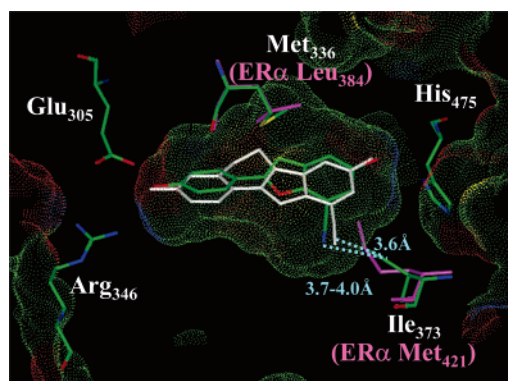

Figure 5. WAY-358 (white) docked to the ERβ/WAY-697 pocket (ligand and residues colored by atom type), overlaid with ERα/DES (magenta, ligand not shown). Only key residues, including a Connolly surface of the ERβ/WAY-697 binding site, are shown for simplicity. Distance monitors show that the nitrile group of WAY-358 is shifted closer to the ERα Met$_{421}$ → ERβ Ile$_{373}$ residue substitution.

evaluated with docking calculations, and functional groups were chosen based on fit to the pocket, likelihood of the group having a differential interaction with methionine versus isoleucine, and synthetic accessibility.

The first strategy resulted in the design of WAY-358, a 157-fold ERβ selective molecule. Figure 5 shows WAY-358 docked to the ERβ/WAY-697 binding site. Clearly, the nitrile of WAY-358 is directed more deeply into the ERα Met$_{421}$/ERβ Ile$_{373}$ pocket relative to WAY-697. Furthermore, due to the conformational constraint, the nitrile is likely to spend a greater percentage of time near these residues, which should magnify the effect of its differential interaction with ERα Met$_{421}$ relative to ERβ Ile$_{373}$ (although alignment of the nitrile with respect to these residues is most likely still far from optimal). As a result, the ERα potency is reduced relative to that of WAY-697, while the ERβ potency is slightly improved. We point out that WAY-358 appears shifted in the pocket relative to WAY-697, which is primarily due to steric interactions between the constraining ethyl moiety and the pocket residues. Therefore, both the constrained ligand geometry and the shift in the pocket should be considered responsible for positioning the nitrile closer to the ERα Met$_{421}$ → ERβ Ile$_{373}$ residue substitution.

Two analogues were designed utilizing the second strategy: WAY-244, a benzofuran with a 7-acetonitrile group, and WAY-659, a benzoxazole with a 7-vinyl group. The 76-fold ERβ selectivity of WAY-244 appears primarily due to a decrease in ERα potency, which is consistent with the positioning of the nitrile nitrogen more deeply in the pocket relative to WAY-697. However, the improvement in selectivity is still modest compared to that of WAY-358. One possible reason for this is that the acetonitrile group is somewhat strained in the ERβ structure, leading to a slight reduction in ERβ affinity as well. In addition, we feel that the nitrile of WAY-244 may still not be optimally aligned to take advantage of the differential interaction we predict with ERα Met$_{421}$ relative to ERβ Ile$_{373}$ (see Figure 4b). This will be discussed further below. Analogue WAY-659 is 127-fold ERβ selective, which is the result of an approximately 16-fold improvement in the ERβ affinity, along with a 3-fold improvement in the ERα affinity (affinities relative to those of WAY-818). The improvement in affinity for both isoforms is most likely due to a favorable overall hydrophobic effect, although the significantly smaller improvement in the ERα potency is consistent with the "nonattractive" potential we

---

(68) Even for this "T-like" relative orientation, we find that the interaction between dimethyl sulfide and acetonitrile is about the same as the interaction between propyl and acetonitrile, given the same intermolecular distance.
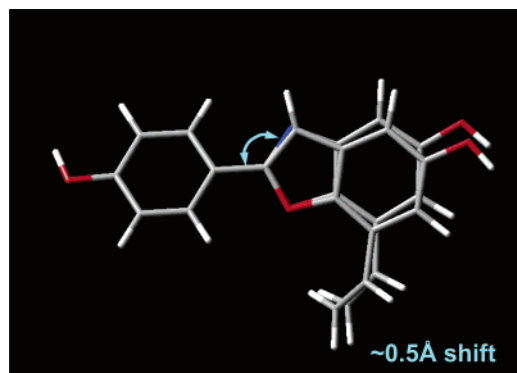
Figure 6. B3LYP/6-31G(d,p) geometries of WAY-659 and WAY-354, overlaid by minimizing the RMSD of the phenol heavy atoms. The A−B ring dihedral angles were both constrained to 23°, and the vinyl dihedral angles were both constrained to 38° with respect to the benzofuran/ benzoxazole plane, to most closely mimic the bound conformation of ERB-041 (see text and Figure 7 below). For ligands with simple unsubstituted phenols, the A-ring overlap is very good when our ERβ crystal structures are overlayed by C_α atoms, consistent with the fact that the A-ring interaction with Glu$_{305}$ and Arg$_{346}$ is critical for binding. However, we emphasize that the "perfect" A-ring overlap shown here is not intended to mimic the overlaying of crystal structures. The purpose of this figure is to highlight the subtle structural differences between the benzofuran and benzoxazole scaffolds, providing one possible explanation for divergences in SAR. The shift of the 7-vinyl group is primarily due to an opening up of the bond angle shown.

predict between the 7-vinyl group and ERα Met$_{421}$, relative to a weak attraction with ERβ Ile$_{373}$.

Interestingly, although the corresponding 7-vinyl benzofuran WAY-354 has a nearly identical ERβ potency, the ERα potency is approximately 5-fold better, leading to a 6-fold *less* selective compound. This can be rationalized by overlaying WAY-659 with WAY-354, shown in Figure 6. One can see from this overlay that there is a subtle difference in scaffold geometry, primarily due to opening up of the benzofuran−phenyl bond angle shown in Figure 6, which in turn is probably a result of steric repulsion between the ortho hydrogen atoms and the larger size of the sp^2 carbon at the benzofuran 3-position relative to the corresponding benzoxazole nitrogen. Although this difference seems small, it leads to a shift of as much as 0.5 Å in the 7-vinyl atomic positions. Given the sensitivity of the interaction energy to intermolecular separation at close distances, we speculate that this shift could readily lead to a 5-fold change in ERα affinity, which corresponds to a free energy difference of only 0.95 kcal/mol. A similar divergence in SAR was seen for the acetonitrile group (data not shown), except in this case the ERβ and ERα potencies were both reduced for the benzoxazole scaffold relative to the benzofuran scaffold.

As mentioned above, selectivities greater than 100-fold were only observed for functional groups capable of forming a differential electronic interaction with the ERα Met$_{421}$ side chain relative to the purely aliphatic side chain of ERβ Ile$_{373}$. Groups that do not experience a significant differential interaction (e.g., aliphatic groups) in the same pocket typically lead to either lesser or no improvement, or sometimes even a detrimental effect on ERβ selectivity. For example, a 7-ethyl group, which was confirmed to occupy the ERβ Ile$_{373}$ pocket by cocrystallization studies, led to no significant change in selectivity for either the benzofuran or benzoxazole scaffold.[35]

Fluoro Group Ortho to A-Ring Hydroxyl Enhances ERβ Selectivity. Traditional medicinal chemistry SAR studies took
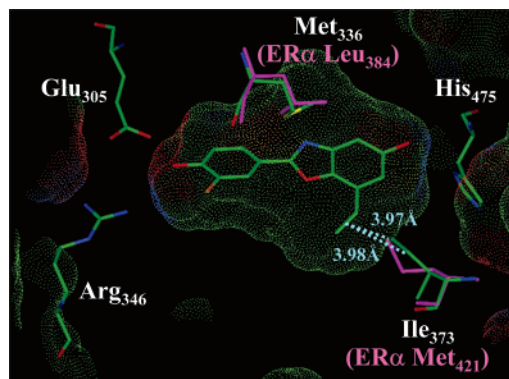
Figure 7. ERβ complexed with ERB-041 (colored by atom type), overlaid with ERα/E2 (magenta, ligand not shown, 1GWR). Only key residues, including a Connolly surface of the ERβ/ERB-041 binding site, are shown for simplicity. Distance monitors show the proximity of the 7-vinyl group to the ERα Met$_{421}$/ERβ Ile$_{373}$ pocket.

Table 3. Lower (LCL) and Upper (UCL) Confidence Limits for the Mean 2-Fold Selectivity Ratio Found When Comparing ERB-041 and WAY-659, Calculated Using the Pooled Variance Method Described in the Text

confidence level (%)	LCL	UCL
80	1.57	2.57
95	1.37	2.94
99	1.21	3.34
99.9	1.04	3.89

WAY-659 to development candidate ERB-041,[7,35] which has a geometric mean ERβ selectivity of 256-fold.[69] An X-ray structure of ERβ complexed with ERB-041 confirmed that the 7-vinyl group does indeed extend into the ERα Met$_{421}$/ERβ Ile$_{373}$ pocket, as shown in Figures 2d and 7. Interestingly, ERB-041 is 2-fold more selective than WAY-659, yet it differs from WAY-659 by only a single fluoro group ortho to the A-ring hydroxyl. We have also observed this selectivity enhancement for ortho-fluoro substituents on other scaffolds as well.[15,37] Although estrogen receptor binding in general is known to be tolerant of A-ring halogen substitution,[70] to our knowledge there have been no other reports of any effects on ERβ/ERα selectivity.

The selectivity improvement for ERB-041 relative to WAY-659 is primarily due to a 2.7-fold reduction in ERα potency. We point out that although the effect of the ortho-fluoro group on ERβ selectivity is small, it is indeed statistically significant at up to 99% confidence, as shown in Table 3. However, the mechanism behind the ERα potency reduction and the resulting selectivity change is difficult to understand, since the X-ray structure of ERβ complexed with ERB-041 reveals that the residues closest to the fluorine atom (Leu$_{343}$, Met$_{340}$, and Leu$_{339}$) are conserved when comparing ERα to ERβ. One possibility may be that the fluorine is only ~2.8 Å from the carbonyl oxygen of Leu$_{339}$, which represents a repulsive interaction.[71]

(69) As discussed in the Materials and Methods section, we chose to work with geometric mean values in order to obtain confidence intervals for the difference between selectivities on a logarithmic scale. However, to avoid confusion with previously reported results, we point out that the selectivity of ERB-041 based on the ratio of arithmetic mean potency values is actually 226-fold.
(70) Anstead, G. M.; Carlson, K. E.; Katzenellenbogen, J. A. *Steroids* **1997**, *62*, 268−303.
(71) We point out that the alternative position of the fluorine atom would place it in close proximity to the carboxylic acid of Glu$_{305}$, which would represent an even stronger repulsive interaction.
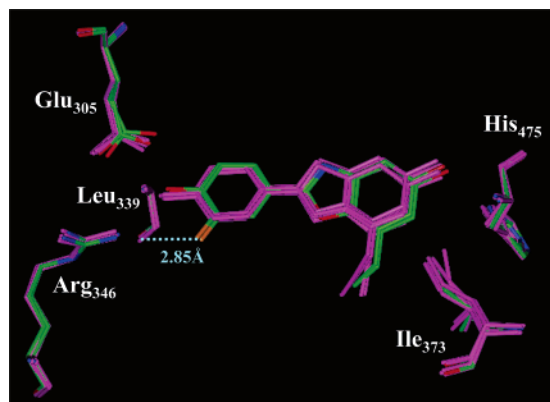
Figure 8. ERβ complexed with ERB-041 (colored by atom type), overlaid with ERβ/WAY-244, ERβ/WAY-697, and ERβ/WAY-397 (magenta). Only key residues are shown for simplicity. The ligands and residues from both monomer units are shown. The close proximity of the ERB-041 fluoro group and the backbone carbonyl of Leu$_{339}$ appears to shift the ligand scaffold slightly relative to the others, placing the 7-vinyl group closer to the ERα Met$_{421}$ → ERβ Ile$_{373}$ residue substitution.

Upon overlay of the ERβ/ERB-041 structure with the other ERβ structures discussed above, it appears that this repulsion shifts the A-ring by up to ∼0.45 Å, as shown in Figure 8. Once the shift has occurred, the remaining repulsion is probably offset by the electron-withdrawing nature of the fluorine, which would tend to polarize the phenolic OH group and improve the interaction with Glu$_{305}$ and Arg$_{346}$. However, the shift also tends to position the 7-vinyl group more deeply into the ERα Met$_{421}$/ERβ Ile$_{373}$ pocket. Given that a 2-fold change in selectivity corresponds to only a 0.4 kcal/mol free energy difference, it is quite reasonable to expect that such a small shift could be responsible for the selectivity improvement. This is not unlike the shift of WAY-358 relative to WAY-697 discussed above. It is also possible that the shift modulates the differential interaction between the B-ring and ERβ Met$_{336}$ relative to ERα Leu$_{384}$.

An ERβ-Selective Ligand Cocrystallized with ERα. To further understand the mechanism for enhancing ERβ selectivity in this series, we cocrystallized WAY-244 with ERα. Despite the relatively low resolution of the structure, we felt that the electron density difference maps were adequate to make some general conclusions about the ligand binding mode (see Figure 2e). First, overlaying the structures of ERα and ERβ, both complexed with WAY-244, reveals that the binding mode is essentially identical in both isoforms, as shown in Figure 9. The B-ring (furan) is approximately 4.2 Å from ERβ Met$_{336}$ C$_ε$, which is about 2 Å closer than the distance to ERα Leu$_{384}$ C$_{δ1}$. This difference serves to highlight the better contact between the B-ring and ERβ Met$_{336}$ relative to ERα Leu$_{384}$, which we propose contributes significantly to what we term the "core selectivity" seen for compounds containing bicyclic heteroaryl groups in the B–C ring region of the ligand,[14,23–26] as well as for biphenyls.[15] However, for the purposes of the current paper, we intend to focus on the mechanism by which certain functional groups *enhance* ERβ selectivity relative to the core scaffold.[72] Therefore, we defer a discussion on the exact

---

(72) Based on quantum chemical calculations similar to those presented in this paper, we find that the B-ring is able to interact more favorably with ERβ Met$_{336}$ relative to ERα Leu$_{384}$. A detailed explanation of this contribution to "core selectivity" will be presented elsewhere.
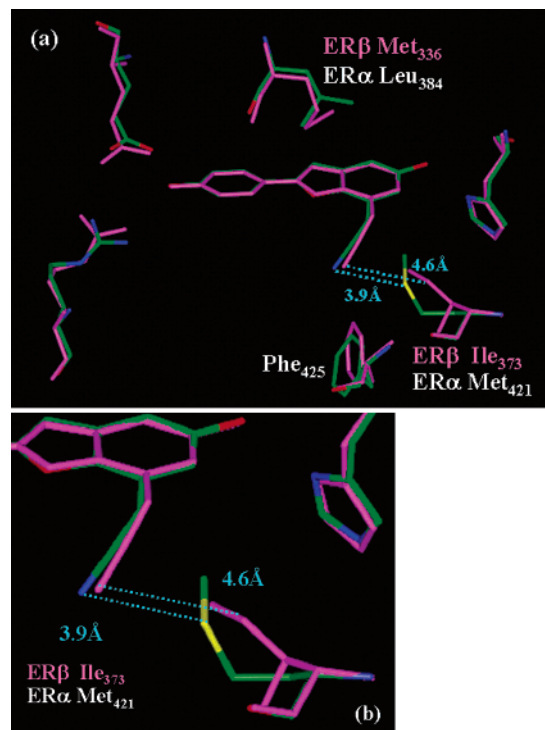

Figure 9. (a) ERα complexed with WAY-244 (colored by atom type), overlaid with ERβ/WAY-244 (magenta). Only key residues are shown for simplicity. Distance monitors show the proximity of the 7-acetonitrile group to ERα Met$_{421}$/ERβ Ile$_{373}$. Interaction with Phe$_{425}$/Phe$_{377}$ appears to induce a strained acetonitrile conformation in both structures. In ERα, we hypothesize that this strain may increase slightly to achieve a more optimal interaction with Met$_{421}$. Interaction between the acetonitrile and Phe$_{425}$ may also be affected by the presence of Met$_{421}$. Part b shows a close-up view of the interaction between the 7-acetonitrile group and ERα Met$_{421}$/ERβ Ile$_{373}$.

mechanism and magnitude of this contribution to core selectivity to an upcoming paper.

Although we feel confident that the acetonitrile group does indeed occupy the ERα Met$_{421}$/ERβ Ile$_{373}$ pocket, the low resolution of the ERα/WAY-244 structure makes it difficult for us to say anything conclusive about the exact mechanism of selectivity enhancement. Fortunately, knowing that the acetonitrile occupies the same pocket in both isoforms in roughly the same conformation does allow us to form several hypotheses regarding how this functional group leads to enhanced ERβ selectivity. The most obvious mechanism would be any direct differential interaction of the acetonitrile with ERα Met$_{421}$ relative to ERβ Ile$_{373}$, given the close proximity of these moieties. Considering the observed intermolecular distances shown in Figure 9, one might think that the differential interaction we predict between the nitrile and ERα Met$_{421}$ relative to ERβ Ile$_{373}$ (see Figure 4b) would be capable of contributing as much as ∼20-fold to the ERβ selectivity. However, based on the observed relative orientations of these moieties, this contribution is likely to be greatly diminished, consistent with the limited improvement in ERβ selectivity for WAY-244 relative to WAY-397. Another contribution we considered is that ERα Met$_{421}$ interferes with the interaction between acetonitrile and Phe$_{425}$, whereas in ERβ the acetonitrile can form a weak CH- - -N hydrogen bond with Phe$_{377}$ (see Figure 9).

Interestingly, the acetonitrile group appears significantly strained in both the ERα and ERβ structures. The primary reason for this appears to be steric interactions with ERα Phe$_{425}$/ERβ

Phe$_{377}$, which is also what prevents the acetonitrile from being optimally aligned to take maximal advantage of the ERα Met$_{421}$ $\rightarrow$ ERβ Ile$_{373}$ residue substitution. This observation is consistent with the reduced affinity of WAY-244 for both isoforms relative to WAY-397. Given that we expect the ligand energy to be more sensitive to small changes in geometry when the ligand is strained compared to when the ligand geometry is at an energy minimum, we considered the possibility that differences in strain energy might contribute to ERβ selectivity. We hypothesize that any additional strain induced in ERα is due to repulsion between the Met$_{421}$ side chain and the acetonitrile group. For example, the C$_{7a}$–C$_7$–C$_{sp3}$–C$_{sp}$ dihedral angle is about 60° in the ERβ structure and about 50° in the ERα structure. This small movement is clearly beyond the resolution of the structures, so we stress that this only represents a starting point to examine the effect of subtle changes in the average ligand geometry. According to quantum chemical calculations,[73] the strain energy corresponding to a dihedral angle of 50° is greater than that corresponding to a dihedral angle of 60° by about 0.5 kcal/mol. This energy difference corresponds to a ~2.3-fold relative potency shift, which would represent a substantial contribution to the 2.7-fold improvement in selectivity observed for WAY-244 relative to WAY-397. Thus, even if the acetonitrile is oriented with respect to ERα Met$_{421}$ such that the repulsion between the two moieties is completely eliminated, it is reasonable to expect that the resulting increase in ligand strain could contribute significantly to the selectivity.

Discussion

The mechanism by which ERβ selectivity can be achieved is generally not thoroughly explained in the literature. There are only two conservative residue substitutions in the ligand binding pocket: ERβ Met$_{336}$ is substituted by ERα Leu$_{384}$, and ERβ Ile$_{373}$ is substituted by ERα Met$_{421}$. It appears that interactions between ERβ Met$_{336}$ and the benzofuran or benzoxazole ring of the analogues discussed above impart some degree of core selectivity. However, these interactions are unable to produce more than ~30-fold ERβ selectivity on their own. We find that groups targeting the ERα Met$_{421}$ $\rightarrow$ ERβ Ile$_{373}$ residue substitution are capable of enhancing ERβ selectivity. Furthermore, selectivities greater than 100-fold were only observed for functional groups that appear capable of forming a differential electronic interaction with the methionine side chain relative to a purely aliphatic side chain. Groups that do not appear able to form a significant differential interaction (e.g., aliphatic groups) in the same pocket typically lead to either lesser or no improvement, or sometimes even a detrimental effect on ERβ selectivity. A semiquantitative understanding of this differential interaction was provided by quantum chemical calculations, which supported our original hypothesis that chemically hard functional groups containing atoms that carry a partial negative charge would be more likely to experience a repulsive interaction with the chemically soft and electronegative methionine sulfur atom.

Clearly, the flexibility of the functional group and that of the methionine side chain both play a strong role in determining the observed selectivity of the compound. The state of the complex observed in a cocrystal structure should reflect the lowest energy state(s) of the entire system. If a functional group introduced to a ligand scaffold experiences a repulsive interaction with the ERα Met$_{421}$ side chain, then the ligand and/or

---

protein will adjust (if possible) to lower the total energy of the complex. This might consist of the ligand adopting a different binding mode, including changes in position, orientation, and conformation. Likewise, the repulsive interaction might lead to changes in the protein conformation, most likely a change in the rotamer state of the methionine side chain. Since we are considering changes in potency on the order of no more than ~10-fold, corresponding to a binding free-energy change of 1.37 kcal/mol at 25 °C, it is more likely that subtle changes will be observed. For example, we hypothesized that interaction between the acetonitrile group of WAY-244 and the ERα Met$_{421}$ side chain may lead to a slight change in the acetonitrile conformation, which in turn is likely to alleviate any repulsive interaction between the two moieties. However, this subtle conformational change is likely to translate into increased ligand strain, which would lead to a significant decrease in ERα binding affinity relative to ERβ. Unfortunately, due to the presence of ERα Phe$_{425}$/ERβ Phe$_{377}$, the acetonitrile is unable to align itself to take optimal advantage of the differential interaction we predict with ERα Met$_{421}$ relative to ERβ Ile$_{373}$. Thus we obtain only a modest improvement in ERβ selectivity for the acetonitrile.

For WAY-659 and ERB-041, differential interaction of the vinyl functional group with a methionine versus aliphatic side chain is predicted to be somewhat small compared to that of acetonitrile. In fact, the difference between the two curves shown in Figure 4c reaches a maximum of 0.98 kcal/mol at an intermolecular separation of 3.8 Å. Based on the crystal structure of ERβ complexed with ERB-041, it is clear that the vinyl group fits tightly into a groove formed by the side chains of residues Ile$_{373}$, Ile$_{376}$, and Phe$_{377}$, and thus there is not much room for the vinyl group to move with respect to ERβ Ile$_{373}$, and most likely with respect to ERα Met$_{421}$ as well. Interestingly, the distance from the ethylene centroid to ERβ Ile$_{373}$ C$_{\gamma1}$ is about 4.0 Å, very close to the distance at which the differential interaction between methionine and isoleucine is predicted to be a maximum. If ERα Met$_{421}$ adopts a rotamer similar to that observed in the ERα/E2 or ERα/WAY-244 crystal structures (see Figure 7), then the 0.98 kcal/mol difference in interaction energy will be maintained, apart from a small zero-point energy correction. Since it only takes about this much energy to take a 24-fold selective molecule like WAY-818 to a 127-fold selective molecule like WAY-659 (a 5.3-fold change in selectivity corresponds to a 0.99 kcal/mol difference in binding free energy), the differential interaction experienced by the vinyl group would be consistent with the observed improvement in selectivity. Thus, although this differential interaction is smaller than the maximum differential interaction we predict for acetonitrile, the vinyl group of WAY-659/ERB-041 is both more optimally aligned and less likely to readjust in order to take maximal advantage of the ERα Met$_{421}$ $\rightarrow$ ERβ Ile$_{373}$ residue substitution. As a result, the vinyl group leads to a greater improvement in selectivity.

It appears that relatively small but statistically significant contributions to the selectivity due to interaction with conserved regions of the binding site may also occur, as was demonstrated with the ortho fluoro substituent of ERB-041. To provide an explanation for this phenomenon, we pointed out that a repulsive interaction between the fluoro group and the backbone carbonyl of Leu$_{339}$ appears to "push" the 7-vinyl group more deeply into the ERα Met$_{421}$/ERβ Ile$_{373}$ pocket and realign the B-ring with respect to ERα Leu$_{384}$/ERβ Met$_{336}$. However, we cannot rule out the possibility that a differential interaction might also occur

---

(73) Calculations were performed at the b3lyp/aug-cc-pVTZ(-f) level of theory.

due to a significant number of residue substitutions outside of the immediate binding site (>5 Å), which in turn affect the equilibrium position and energetics of the backbone carbonyl within the binding pocket. We emphasize that such effects are not direct "long-range" effects, but rather they originate from one or more relatively distant residue substitutions, which propagate to the ligand either by shifting a residue within the binding site in one isoform relative to the other or by making it energetically possible for the ligand to induce such a shift.

For WAY-358, the improvement in selectivity relative to WAY-697 appears to be due to a combination of several factors: a change in equilibrium geometry and increased rigidity associated with the constraining ethyl moiety, and a shift of the ligand due to steric interactions between the ethyl moiety and the pocket residues. This last contribution is similar to our explanation for the mechanism of selectivity enhancement for the ERB-041 fluoro group, except in this case steric interactions between the ethyl bridge and pocket residues Ala_{302} and Leu_{298} cause the shift, rather than electrostatic repulsion between the fluoro group and a backbone carbonyl.

In our discussion of the ERα/WAY-244 crystal structure, we mentioned that the aryl interaction with ERβ Met_{336} in bicyclic heteroaryl scaffolds appears to contribute about an order of magnitude to the baseline selectivity. A logical question to ask is whether such scaffolds take maximal advantage of the ERα Leu_{384} → ERβ Met_{336} residue substitution. For instance, why not attempt to form an additional interaction with ERβ Met_{336}, such as a hydrogen bond to the $S_δ$ atom, since this type of interaction was also found to be responsible for the RARγ selectivity of certain retinoids possessing an alcohol or oxime moiety?[74−79] It turns out that, due to the planar geometry of the bicyclic heteroaryl scaffold, none of the substitutable positions afforded easy access to the ERβ Met_{336} $S_δ$ atom. Furthermore, even if we were able to find another scaffold that presented better opportunities to access ERβ Met_{336}, such hydrogen bonds are expected to be very sensitive to the relative position and orientation of the donor and acceptor. If the interaction is not optimal, desolvation of an alcohol or oxime would thus tend to lower the affinity for both ERα and ERβ. The other option would be to gain an attractive interaction with the ERβ Met_{336} $S_δ$ atom via a soft−soft interaction, similar to the interaction proposed between this residue and DPN[19,20] or between 16α-iodo E2 and ERα Met_{421}.[67] However, we felt that this type of interaction would be unlikely to significantly improve upon the interaction we were already making with our current scaffolds. The benzofuran/benzoxazole scaffold provided the additional opportunity to take advantage of the ERα Met_{421} → ERβ Ile_{373} residue substitution by a combination of both steric and electronic effects, allowing for a much greater potential to develop SAR with a variety of functional groups.

Our goal of designing an ERβ selective *agonist* added another level of difficulty to the simpler problem of designing an ERβ selective *ligand*. The observation that ERβ is easier to antagonize than ERα further complicates the design process.[14] The

approach we chose to address this issue was to design ligands within the confines of an "agonist-like" pocket, in which helix-12 is closed over the binding cavity as described above. Earlier crystallography studies indicated that helix-12 of ERβ maintains an agonist-like conformation when WAY-397 is bound to the receptor, regardless of whether a coactivator peptide fragment was utilized in the crystallization process[80] (this is in contrast to the behavior of ERβ complexed with GEN, where helix-12 adopts an antagonist-like conformation in the absence of a coactivator peptide fragment[14]). In addition, the results of a cell-based transcriptional assay[7] measuring up-regulation of insulin-like growth factor binding protein-4 mRNA indicate that WAY-397 behaves as both an ERβ and ERα agonist. This suggested to us that the ligand binding pocket of ERβ/WAY-397 was a good starting point for structure-based design. Likewise, ERβ complexed with the final development compound ERB-041 also showed that helix-12 continued to adopt an agonist-like conformation, allowing for the binding of a coactivator fragment. Again, this is consistent with the fact that ERB-041 behaves as a full agonist on ERβ and ERα[7]. We emphasize that this only demonstrates that the structures are *consistent* with the observed functional activity of the compounds. However, one should not generally expect the position of helix-12 to be fully predictive of functional activity, since other factors such as the binding of the coactivator fragment itself and crystal packing also make a contribution to the overall energetics of the crystal. Ultimately, we feel that the helix-12 conformation should only be used to provide a structural basis for why a compound may have reduced functional efficacy (i.e. partial agonist) or full antagonist behavior. In our case there was no issue, since the compounds of interest demonstrated not only ERβ selectivity but also an agonist-like helix-12 conformation, consistent with their measured functional activity.

Conclusions

In conclusion, we have demonstrated that structure-based design affords ligands with >100-fold ERβ selectivity relative to ERα. Multiple X-ray cocrystal structures of modestly selective ligands complexed to both ERα and ERβ, in conjunction with docking calculations, were utilized to take advantage of a single conservative residue substitution in the ligand binding pocket, ERα Met_{421} → ERβ Ile_{373}, to optimize ERβ selectivity. Quantum chemical calculations were also used to provide an understanding of how certain functional groups might experience a differential interaction with ERβ Ile_{373} relative to ERα Met_{421}. These structure-based design methods have helped lead to the discovery of compounds such as ERB-041, a >200-fold ERβ selective agonist,[7] providing a tool to elucidate the physiological role of ERβ.

(74) Charpentier, B.; Bernardon, J. M.; Eustache, J.; Millois, C.; Martin, B.; Michel, S.; Shroot, B. *Journal of Medicinal Chemistry* **1995**, *38*, 4993−5006.
(75) Klaholz, B. P.; Mitschler, A.; Moras, D. *Journal of Molecular Biology* **2000**, *302*, 155−170.
(76) Egea, P. F.; Klaholz, B. P.; Moras, D. *FEBS Letters* **2000**, *476*, 62−67.
(77) Klaholz, B. P.; Moras, D. *Pure and Applied Chemistry* **1998**, *70*, 41−47.
(78) Klaholz, B. P.; Renaud, J. P.; Mitschler, A.; Zusi, C.; Chambon, P.; Gronemeyer, H.; Moras, D. *Nature Structural Biology* **1998**, *5*, 199−202.
(79) Klaholz, B.; Moras, D. *Structure* **2002**, *10*, 1197−1204.

(80) Manas, E. S. Unpublished observations.
(81) Laskowski, R. A.; MacArthur, M. W.; Moss, D. S.; Thornton, J. M. *Journal of Applied Crystallography* **1993**, *26*, 283−291.